Mechanism of a GatCAB Amidotransferase: Aspartyl-tRNA Synthetase Increases Its Affinity for Asp-tRNA^{Asn} and Novel Aminoacyl-tRNA Analogues Are Competitive Inhibitors†

Jonathan L. Huot,‡ Christian Balg,§ Dieter Jahn,|| Jürgen Moser,|| Audrey Émond,‡ Sébastien P. Blais,‡ Robert Chênevert,§ and Jacques Lapointe*,‡

Centre de Recherche sur la Fonction, la Structure et l'Ingénierie des Protéines, Département de Biochimie et de Microbiologie, et Département de Chimie, Université Laval, Québec, Québec, Canada G1K 7P4, and Institute of Microbiology, Technical University Braunschweig, Spielmannstrasse 7, D-38106 Braunschweig, Germany

Received March 29, 2007; Revised Manuscript Received August 29, 2007

ABSTRACT: The trimeric GatCAB aminoacyl-tRNA amidotransferases catalyze the amidation of Asp-tRNA^{Asn} and/or Glu-tRNA^{Gln} to Asn-tRNA^{Asn} and/or Gln-tRNA^{Gln}, respectively, in bacteria and archaea lacking an asparaginyl-tRNA synthetase and/or a glutaminyl-tRNA synthetase. The two misacylated tRNA substrates of these amidotransferases are formed by the action of nondiscriminating aspartyl-tRNA synthetases and glutamyl-tRNA synthetases. We report here that the presence of a physiological concentration of a nondiscriminating aspartyl-tRNA synthetase in the transamidation assay decreases the K_m of GatCAB for Asp-tRNA^{Asn}. These conditions, which were practical for the testing of potential inhibitors of GatCAB, also allowed us to discover and characterize two novel inhibitors, aspartycin and glutamycin. These analogues of the 3′-ends of Asp-tRNA and Glu-tRNA, respectively, are competitive inhibitors of the transamidase activity of *Helicobacter pylori* GatCAB with respect to Asp-tRNA^{Asn}, with K_i values of 134 μM and 105 μM, respectively. Although the 3′ end of aspartycin is similar to the 3′ end of Asp-tRNA^{Asn}, this analogue was neither phosphorylated nor transamidated by GatCAB. These novel inhibitors could be used as lead compounds for designing new types of antibiotics targeting GatCABs, since the indirect pathway for Asn-tRNA^{Asn} or Gln-tRNA^{Gln} synthesis catalyzed by these enzymes is not present in eukaryotes and is essential for the survival of the above-mentioned bacteria.

The specific aminoacylation of tRNAs is at the center of the faithful translation of nucleic acid sequence information into proteins. This process involves mainly the aminoacyl-tRNA synthetases (aaRS)[1] but also enzymes involved in the editing or maturation of aminoacyl-tRNAs whose aminoacyl moiety does not correspond to the anticodon moiety according to the genetic code [reviewed by Ataide and Ibba (*1*)]. Some of these misacylated tRNAs are deacylated by editing domains present in certain aaRSs or by free deacylases (refs *2* and *3* and references therein), whereas others are modified on their aminoacyl moiety. The aminoacyl-tRNA amidotransferase (AdT) (*4*) is such a modifying enzyme used in the indirect pathway of Gln-tRNA^{Gln} and/or Asn-tRNA^{Asn} biosynthesis from Glu-tRNA^{Gln} and/or Asp-tRNA^{Asn}, in archaea and bacteria that lack the aminoacyl-tRNA synthetases specific for glutamine (GlnRS) and/or asparagine (AsnRS). The misacylated Glu-tRNA^{Gln} and Asp-tRNA^{Asn}, which are substrates of AdT, are synthesized by nondiscriminating glutamyl-tRNA synthetases (ND-GluRS) and aspartyl-tRNA synthetases (ND-AspRS), respectively, which also charge glutamic acid and aspartic acid onto tRNA^{Glu} and tRNA^{Asp}, respectively. This indirect pathway of Asn-tRNA^{Asn} synthesis is also used for the biosynthesis of free asparagine in organisms such as *Thermus thermophilus* and *Deinococcus radiodurans*, which have an AsnRS but no asparagine synthetase (*5*−*7*), and in *Bifidobacterium longum*, where asparagine synthetases (AsnA and AsnB) and AsnRS are absent (*8*).

Two types of AdT have been found: a trimeric one (GatCAB), present in most bacteria and some archaea, can use both Glu-tRNA^{Gln} and Asp-tRNA^{Asn} as substrates, whereas a dimeric GatDE, present only in archaea, uses only Glu-tRNA^{Gln} [reviewed by Ibba et al. (*9*)]. The crystallographic structures of members of each type have been determined recently (*10*−*12*). In this work, we have tested the influence of two analogues of the 3′ end of Asp-tRNA

† This work has been supported by Grant OGP0009597 from the Natural Sciences and Engineering Research Council of Canada (NSERC) to J.L. and Grant PR- 105092 from the Fond de Recherche sur la Nature et les Technologies du Québec (FQRNT) to J.L. and R.C.

* Address correspondence to this author: phone (418) 656-2131, ext 3411; fax (418) 656-3664; e-mail Jacques.Lapointe@bcm.ulaval.ca.

‡ Centre de Recherche sur la Fonction, la Structure et l'Ingénierie des Protéines, Département de Biochimie et de Microbiologie, Université Laval.

§ Centre de Recherche sur la Fonction, la Structure et l'Ingénierie des Protéines, Département de Chimie, Université Laval.

|| Technical University Braunschweig.

[1] Abbreviations: AdT, amidotransferase; Asp-tRNA, aspartyl-tRNA^{Asn} and/or aspartyl-tRNA^{Asp}; Asn-tRNA, asparaginyl-tRNA^{Asn}; Glu-tRNA, glutamyl-tRNA^{Gln} and/or glutamyl-tRNA^{Gln}; Gln-tRNA, glutaminyl-tRNA^{Gln}; ND-AspRS, nondiscriminative aspartyl-tRNA synthetase; AsnRS, asparaginyl-tRNA synthetase; GluRS, glutamyl-tRNA synthetase; GlnRS, glutaminyl-tRNA synthetase; aaRS, aminoacyl-tRNA synthetase; aa-tRNA, aminoacyl-tRNA; LCMS, liquid chromatography/mass spectrometry.

10.1021/bi700602n CCC: $37.00
Published on Web 10/11/2007

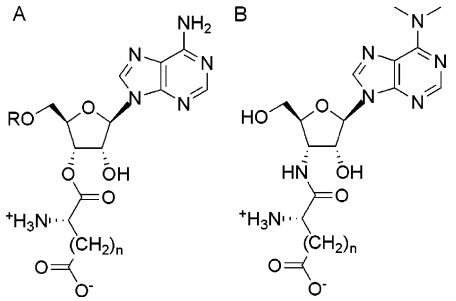

FIGURE 1: AdT aminoacyl-tRNA substrates and analogues. (A) Asp-tRNA^{Asn} when $n = 1$ and Glu-tRNA^{Gln} when $n = 2$: tRNA continues past the terminal adenosine at R. (B) Glutamycin and aspartycin, analogues of Glu-tRNA and Asp-tRNA, respectively. This figure represents glutamycin when $n = 2$ and aspartycin when $n = 1$. The terminal adenosine of the substrate is kept, with only the replacement of two hydrogen atoms by two methyl groups, and the ester bond between the tRNA and the amino acid is replaced by an amide bond.

and of Glu-tRNA on the transamidation activity of the trimeric AdT of *Helicobacter pylori*, a Gram-negative bacteria that has neither AsnRS nor GlnRS (*13*). This GatCAB, as well as those characterized from other bacteria or archaea, can use as substrate in vitro either Glu-tRNA^{Gln} or Asp-tRNA^{Asn}. Whether a GatCAB amidotransferase performs one or both of these functions inside a cell is related to the presence or absence of GlnRS, AsnRS, and asparagine synthetase.

The presence of a trimeric AdT in most bacteria, and the absence of either dimeric or trimeric AdT in the cytoplasm of eukaryotes, identify GatCAB as a promising target for the development of new types of antibiotics. Moreover, Gln-tRNA^{Gln} and Asn-tRNA^{Asn} synthesis in mitochondria of *Saccharomyces cerevisiae*, and possibly of all eukaryotes, are catalyzed by a GlnRS and an AsnRS, respectively [*14*; reviewed by Ataide and Ibba (*1*) and by Kern et al. (*15*)]. Therefore, AdT inhibitors will target protein biosynthesis in the above-mentioned bacteria, without affecting it in mammalian cytoplasm or mitochondria.

So far, few AdT inhibitors have been developed, in part because of the absence of a convenient assay. Some analogues of ATP and glutamine inhibit AdT and were useful to study its mechanism (*16*−*18*); however, as these analogues will likely interfere with several other enzymatic processes within mammalian cells, they cannot be lead compounds for the design of novel antibiotics. These studies included the first thorough kinetic analyses of AdT, yielding K_m values for glutamine and ATP and an estimate of the K_m for Glu-tRNA^{Gln}. In our search for inhibitors specific to AdT, we looked for analogues of the 3′ ends of its aa-tRNA substrates; one of them, glutamycin (Figure 1), is a puromycin analogue that is a weak inhibitor of glutamyl-tRNA^{Glu} reductase, the first enzyme of the tRNA-dependent tetrapyrrole biosynthesis pathway (*19*). Having noticed that instability of the AdT substrates and products could be a handicap for the kinetic characterization of this and other inhibitors of the transamidation reaction, we chose conditions that could minimize the effect of any deacylation. In doing so, we found evidence of Asp-tRNA^{Asn} channeling between the ND-AspRS that synthesizes it and the GatCAB AdT that uses it as a substrate. We also report here the characterization of the two first AdT

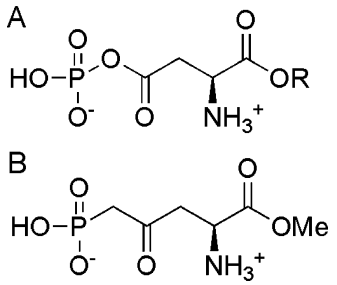

FIGURE 2: (A) β-Phosphoryl-aspartyl-tRNA^{Asn}, a reaction intermediate in transamidation. Shown here is the amino acid portion alone, with R indicating the position of the tRNA. (B) Asp-KP, a stable analogue of a part of β-phosphoryl-aspartyl-tRNA^{Asn}. The activating phosphate is replaced by a stable phosphonate group, while tRNA is entirely replaced by a methyl group.

inhibitors competitive with respect to their misacylated aa-tRNA substrates.

MATERIALS AND METHODS

General Information on Inhibitor Synthesis. Chemical reagents were purchased from Aldrich−Sigma Chemical Co. except for *N*-Boc-L-aspartic acid β-*tert*-butyl ester (Novabiochem). Flash column chromatography was carried out on 40−63 μM (230−400 mesh) silica gel. Reverse-phase HPLC was performed on a Hewlett-Packard 1050 liquid chromatograph (Vydac C_{18} column). Optical rotations were measured on a Jasco DIP-360 digital polarimeter (concentration as grams of compound per 100 mL). Infrared spectra were recorded on a Bomem MB-100 spectrometer. NMR spectra were recorded on a Varian Inova AS400 spectrometer (400 MHz). (*R*)-4-Oxo-5-phosphononorvaline methyl ester (Asp-KP) (Figure 2) was synthesized in three steps from L-aspartic acid dimethyl ester hydrochloride according to a known procedure (*20*). Synthesis of 3′-deoxy-N^6,N^6-dimethyl-3′-(L-glutamylamido)adenosine (glutamycin) (Figure 1) has already been published (*21*).

Synthesis of 3′-Deoxy-N^6,N^6-dimethyl-3′-(N^α-Boc-β-tert-butyl-L-aspartyl-amido)adenosine (Aspartycin Synthesis Intermediate). A suspension of 3′-amino-3′-deoxy-N^6,N^6-dimethyladenosine (puromycin aminonucleoside; 40.0 mg, 136 μmol) in anhydrous *N*,*N*-dimethylformamide (DMF) (1.2 mL) was added to *N*-Boc-L-aspartic acid β-*tert*-butyl ester (43.3 mg, 150 μmol), *N*-hydroxysuccinimide (25.8 mg, 224 μmol), and *N*-(3-dimethylaminopropyl)-*N*′-ethylcarbodiimide hydrochloride (EDC) (33.2 mg, 173 μmol). The mixture was stirred at 0 °C for 30 min and then at room temperature for 24 h. The solvent was coevaporated with toluene and the residue was purified by flash chromatography (4% MeOH/CH_2Cl_2) to give the coupling product (65.5 mg, 85%) as a white solid: mp 96−98 °C; $[\alpha]_D^{21}$ −35.5 (*c* 1.14, MeOH); IR (KBr) 3408, 2979, 2933, 1721, 1671, 1602, 1368, 1162, 1039 cm^{-1}; ^{1}H NMR (400 MHz, CD_3OD) δ 1.42 (s, 18H), 2.54 (dd, $J = 16.0$, 7.9 Hz, 1H), 2.74 (dd, $J = 16.1$, 5.9 Hz, 1H), 3.42 (br s, 6H), 3.71 (dd, $J = 12.5$, 2.9 Hz, 1H), 3.90 (dd, $J = 12.5$, 1.6 Hz, 1H), 4.12−4.18 (m, 1H), 4.47 (t, $J = 6.9$ Hz, 1H), 4.53−4.62 (m, 2H), 5.98 (d, $J = 2.1$ Hz, 1H), 8.12 (s, 1H), 8.30 (s, 1H); ^{13}C NMR (100 MHz, CD_3OD) δ 27.1, 27.5, 37.4, 37.9, 50.8, 51.5, 61.2, 73.9, 79.8, 81.2, 84.0, 90.8, 120.3, 138.0, 149.2, 151.7, 154.8, 156.5, 170.2, 172.9; HRMS (ESI) calcd for $C_{25}H_{39}N_7O_8$ $(M + H)^+$ 566.2933, found 566.2945.

*Synthesis of 3′-Deoxy-N^6,N^6-dimethyl-3′-(*L*-aspartyl-amido)adenosine (Aspartycin).* A solution of the previously prepared compound (40.0 mg, 70.7 μmol) in trifluoroacetic acid (1.0 mL) was stirred at room temperature for 12 min. The solvent was coevaporated under reduced pressure with CH_3CN at 35 °C. The solid residue was dissolved in a minimum of MeOH (2.0 mL) and precipitated by the addition of Et_2O (10 mL). After filtration, this crude product was purified by HPLC on reverse phase (C_{18}; 0% to 75% CH_3CN/H_2O). Evaporation of the relevant fractions provided aspartycin (22.3 mg, 77%) as a colorless solid: mp 105−107 (decomp); $[\alpha]_D^{21}$ −4.4 (*c* 0.46, MeOH); IR (KBr) 3430, 2928, 1678, 1604, 1204, 1137, cm^{-1}; ^1H NMR (400 MHz, CD_3OD) δ 2.89 (dd, J = 17.7, 8.1 Hz, 1H), 2.99 (dd, J = 17.7, 4.9 Hz, 1H), 3.59 (br s, 6H), 3.69 (dd, J = 12.6, 2.9 Hz, 1H), 3.91 (dd, J = 12.6, 2.3 Hz, 1H), 4.18 (dt, J = 7.8, 2.4 Hz, 1H), 4.26 (dd, J = 7.9, 5.0 Hz, 1H), 4.58 (dd, J = 5.6, 2.5 Hz, 1H), 4.69 (dd, J = 7.9, 5.7 Hz, 1H), 6.09 (d, J = 2.5 Hz, 1H), 8.27 (s, 1H), 8.51 (s, 1H) ^{13}C NMR (100 MHz, CD_3OD) δ 35.0, 49.8, 50.9, 60.6, 74.2, 83.6, 91.0, 120.2, 139.4, 147.6, 148.2, 151.6, 168.6, 171.4; HRMS (ESI) calcd for $C_{16}H_{23}N_7O_6$ $(M + H)^+$ 410.1783, found 410.1783.

Bacterial Strains and Plasmids. Pseudomonas aeruginosa ADD1976, carrying the pUCPKS plasmid containing the *P. aeruginosa* PAO1 *aspS* gene, was used to produce His-tagged ND-AspRS, as previously described (*22*). *Escherichia coli* DH5 α, carrying the pQE-80L plasmid containing the *H. pylori* ND-AspRS gene, was kindly provided by Professor Tamara Hendrickson (Johns Hopkins University). Plasmid pET15b containing the *gatCAB* operon of *H. pylori* was kindly provided by Professor Dieter Söll (Yale University), and used to transform *E. coli* BL21 (DE3) (Novagen) according to the manufacturer's specifications. *E. coli* XL1-blue, carrying the pGFIB-HptRNA^{Asn} plasmid for overexpression of the *H. pylori* tRNA^{Asn} gene, was also a gift from Professor Söll.

Production of ND-AspRS from P. aeruginosa and H. pylori. ADD1976/pUCPKS-*AspS* growth and *P. aeruginosa* ND-AspRS overproduction and purification by affinity chromatography on nickel−nitrilotriacetate (Ni-NTA) were conducted as previously described (*22*), except that the resin-bound extract was washed successively with 20 and 60 mM imidazole to reduce the amount of contaminants; AspRS was then eluted with 300 mM imidazole and was pure to over 99% homogeneity. *H. pylori* ND-AspRS was produced with *E. coli* DH5α/pQE-80L-*AspS*, as previously described (*23*).

Production of H. pylori GatCAB. E. coli BL21 (DE3)/pET15b-*gatCAB* was grown in LB medium, which was altered to allow overproduction by autoinduction. This medium was prepared by supplementing LB medium with glycerol (0.5%), glucose (0.05%), lactose (0.2%), Na_2HPO_4 (50 mM), KH_2PO_4 (50 mM), and $(NH_4)_2SO_4$ (25 mM), as indicated for ZYP-5052 (*24*). A 1% inoculation was made from a preculture in the exponential growth phase, itself prepared from a recently transformed single colony. Cultures were incubated overnight at 37 °C in the presence of 100 μg/mL ampicillin and harvested by centrifugation. *H. pylori* GatCAB was then purified to over 99% homogeneity by affinity chromatography as described above for ND-AspRS.

Partial Purification of tRNA Enriched with H. pylori tRNA^{Asn}. E. coli XL1-blue/pGFIB-HptRNA^{Asn} was grown in LB medium containing 250 μg/mL ampicillin. Cultures were incubated at 30 °C for 24 h. Cells were then harvested by centrifugation, and unfractionated tRNA was partially purified as previously described (*22*). The tRNA^{Asn} concentration of the resulting stock unfractionated tRNA solution was determined with a transamidation plateau, as described below.

Preparation of Aspartyl-tRNA. Asp-tRNA was formed in the following reaction mixture: 50 mM *N*-(2-hydroxyethyl)-piperazine-*N*′-ethanesulfonic acid (Hepes)-KOH, pH 7, 15 mM $MgCl_2$, 25 mM KCl, 1 mM dithiothreitol (DTT), 2 mM ATP, and 70 μM [^{14}C]aspartic acid (207 mC_i/mmol, GE Healthcare). Unfractionated tRNA was added at a concentration yielding 20 μM tRNA^{Asn}, and *P. aeruginosa* ND-AspRS was added at a concentration of 1 μM. The reaction mixture was incubated at 37 °C for 45 min, before 1 volume of sodium acetate (0.6 M, pH 5.2) was added. The resulting solution was submitted to an acid-buffered (pH 5.2) phenol/chloroform extraction and precipitated with 2.5 volumes of 95% ethanol. After centrifugation, the Asp-tRNA substrate was rinsed twice with 70% ethanol, resuspended in deionized water, and kept on ice for immediate use.

Half-Life Measurements. Purified Asp-tRNA, prepared as described above, was added to the same reaction mixture used for aminoacylation, except that [^{14}C]aspartic acid, ND-AspRS, and unfractionated tRNA were omitted. Reactions mixtures were incubated at 37 °C. Aliquots taken at various intervals were transferred onto 1 cm × 2 cm filter papers (Whatman) and quenched in trichloroacetic acid (5%). The filter papers were then washed and assayed by liquid scintillation counting, as previously described (*22*).

Transamidase Activity Assay. Reaction conditions were the following: 50 mM Hepes-KOH, pH 7, 15 mM $MgCl_2$, 25 mM KCl, 1 mM DTT, 2 mM ATP, and 1.28 mM L-glutamine. Asp-tRNA, prepared as described above, was added to each reaction mixture prior to each experiment. Before addition of GatCAB to the reaction mixture, an aliquot was taken and incubated at 37 °C in the presence of an excess (6.3 μM) of GatCAB for 2 min before being quenched and precipitated as indicated below. Meanwhile, GatCAB (16.4 nM) was added to the main reaction mixture, and aliquots were taken at 15 s intervals and then quenched in 1 volume of 0.6 M sodium acetate, pH 5.2, kept on ice until 2.5 volumes of 95% ethanol could be added, and placed at −80 °C for 30 min. The aliquots were then centrifuged for 30 min at 14000*g*. The supernatant was carefully removed, and the nucleic acid pellets were left to dry for 10 min at room temperature. The precipitate was then resuspended in 10 μL of 50 mM KOH and heated at 65 °C for 8 min to deacylate the aa-tRNA. Pellets were not completely dried, to ensure a more complete resuspension at the next step, nor were they washed in 70% ethanol, in order to minimize aa-tRNA loss. A small amount of each aliquot was then spotted onto a 20 cm × 20 cm cellulose−poly(ethylenimine) (PEI) plate. Migration was done in a 4:1 mixture of ethanol/ammonium hydroxide, inside a chamber that had been allowed to equilibrate for at least 30 min. Migration took approximately 2.5 h, after which the TLC plate was allowed to dry under ventilation. The aliquots that had contained an excess of GatCAB, in which the substrate was completely transamidated, were used to determine the initial Asp-tRNA^{Asn} concentrations in each reaction mixture. Because these values indicated Asp-tRNA^{Asn} concentrations

existing after the preparative phenol/chloroform extraction, they were used for the calculation of kinetic parameters.

Aminoacylation and Transamidation Assay. When aminoacylation and transamidation were performed sequentially in the same reaction mixture, as is the case for transamidation plateau and inhibition experiments, this mixture was composed of 50 mM Hepes-KOH, pH 7, 15 mM $MgCl_2$, 25 mM KCl, 1 mM DTT, 2 mM ATP, 70 μM [^{14}C]aspartic acid (207 mC_i/mmol), and 1.28 mM L-glutamine. The indicated concentrations were reached once the mixture was combined with tRNA and enzymes. The reactions took place at 37 °C, usually in a final volume of 135 μL. tRNA was added at the indicated concentrations. Once ND-AspRS was added to a concentration of 300 nM, reaction mixtures were incubated for 90 min (unless otherwise stated), and then put on ice for 15 min, with inhibitors if indicated. The reaction mixtures, and AdT in 20 mM Hepes-KOH pH 7, were then incubated at 37 °C for 2 min before being combined to start the transamidation reaction. When potential inhibitors were tested, 5−9 nM GatCAB was used, and aliquots were taken at intervals of 20 s, then quenched and treated as described above. When the $tRNA^{Asn}$ concentration of an unfractionated tRNA stock was determined, 250 nM GatCAB was used to rapidly obtain a plateau by taking aliquots at various intervals. In both of these cases, the cellulose−PEI plates were soaked for 2 h in deionized water and then dried at ambient temperature, before use.

TLC Data Analysis. Quantification of the amino acids rests upon the application of a series of radioactivity standard solutions. By use of [^{14}C]aspartic acid, standards were prepared with concentrations of 9, 3, 1, 0.33, 0.11, and 0.037 μM. The precision of this set of standards was confirmed by liquid scintillation counting. After the migration, 1 μL of each standard was spotted onto each TLC plate in duplicate (Figure 3). After drying, the plates were wrapped in a thin plastic membrane (Saran wrap), and then exposed overnight against a phosphorimager plate (FujiFilm). Data were collected from the phosphorimager plate with a Typhoon Imager by use of the ImageQuant software (GE Healthcare). Intensity at each point of interest was measured, and background intensity was subtracted. From the radioactivity standards, a curve was plotted for signal intensity = f (pmol of aspartic acid). This relation was linear ($R^2 > 0.999$) for the entire range of concentrations tested. This curve was then used to convert signal intensity for each point of interest into absolute amino acid quantities.

Nitrocellulose Binding Assay. Nitrocellulose filters, which bind proteins but not nucleic acids, were used to measure what fraction of Asp-tRNA could be retained by various concentrations of *H. pylori* ND-AspRS and GatCAB, and by BSA as a control. The reaction mixtures contained 207 nM Asp-tRNA, which was prepared as described above. Experiments took place under the conditions used for the transamidase activity assay, except that the pH was 7.2 and glutamine was absent to prevent GatCAB from transamidating Asp-tRNA. The nitrocellulose assay was adapted from previous work (*25*, *26*), with 250 μL of reaction mixture for each filter. Tests were performed in duplicate.

Mass Spectrometric Analysis of Aspartycin and Derivatives. Samples were analyzed by liquid chromatography/mass spectrometry (LCMS) on an Agilent 1100 system. A few microliters were injected on a Zorbax 300 SB-C18 narrow-bore 2.1 mm × 150 mm reversed-phase column (particle size 5 μm), protected by a Zorbax 300 SB-C18 analytical guard column 4.6 mm × 12.5 mm (Agilent Technologies, Montréal, Québec, Canada). Separation was carried out at a flow rate of 200 μL/min, delivered by an Agilent 1100 HPLC1 quaternary pump. Mobile phase A was composed of HPLC-grade water containing 0.1% formic acid. A gradient of mobile phase B (HPLC-grade acetonitrile containing 0.1% formic acid) was imposed, starting from 5% up to 0.5 min, increased linearly to 30% at 3.0 min, 70% at 23 min, 98% at 29 min, maintained until 32.5 min, then brought back to 5% at 36 min, and maintained at that value until 52 min. The eluted molecules were monitored by UV absorption at 214, 220, and 280 nm on a diode array detector (Agilent). The autosampler maintained the samples at 4 °C and the column temperature was kept at 40 °C. The molecular mass of purified analytes was determined by an Agilent 1100 MSD ESI mass spectrometer in the positive electrospray ionization mode. The fragmentor and capillary voltages were set at 70 and 3250 V, respectively. Nitrogen was used both as the nebulizer at 20 psig and as the drying gas at a flow rate of 10 L/min and a temperature of 350 °C. The mass spectrometer was operated in full scan mode from 50 to 550 m/z with a step of 0.1 and a cycle time of 1.18 s.

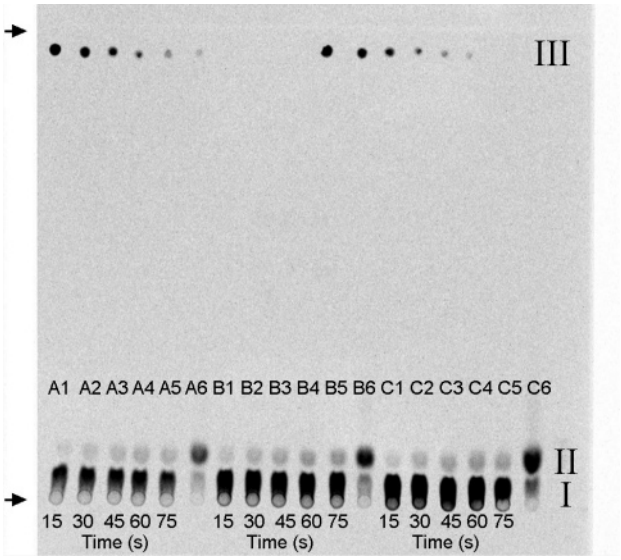

FIGURE 3: An example of the transamidation assay, using Asp/Asn separation by thin-layer chromatography. Reaction mixture aliquots taken at various times were precipitated, resuspensed, deacylated, and dotted onto a 20 × 20 cm sheet of polyester-backed cellulose-PEI at the level indicated by the lower arrow. Separation was done over 2−3 h in a 4:1 ethanol/ammonium hydroxide mixture with the solvent front rising to the upper arrow. Asparagine (II) migrated further than aspartic acid (I). Radioactivity standards were deposited in duplicate (III). In each of the three kinetic reactions shown, Asp-$tRNA^{Asn}$ concentrations were verified as described under Materials and Methods for lanes A6, B6, and C6, which were subjected to a rapid transamidation in the presence of 6.3 μM GatCAB. In these three lanes, we could also see that our Asp-tRNA substrate contained about 4 times more Asp-$tRNA^{Asn}$ than Asp-$tRNA^{Asp}$. Lanes 1−5 of kinetic reactions A, B, and C therefore show the amount of Asn-$tRNA^{Asn}$ formed by 16.4 nM GatCAB, with concentrations of 1.11 μM, 2.43 μM, and 3.93 μM Asp-$tRNA^{Asn}$ as substrate, respectively.

RESULTS

Adapting the [^{14}C]Asp-$tRNA^{Asn}$ Transamidase Assay. The difficulty in developing a satisfying assay for measuring the

kinetic parameters of the tRNA-dependent amidotransferase reaction is highlighted by the fact that the first report of such values (*18*) was published 4 years after the first cloning of an AdT gene, that of *Bacillus subtilis* gatCAB, and the first characterization of this novel heterotrimeric enzyme (*4*). The assay used for these measurements included unlabeled Glu-tRNA^{Gln} as substrate and HPLC analysis of the glutamine released by the deacylation of the aa-tRNA product. These authors indicated that they had obtained only an approximate K_m for Glu-tRNA^{Gln} in the transamidation reaction, because the low concentrations of this substrate needed to obtain a precise value resulted in product concentrations too close to the detection limit of their method.

Since then, and during the preparation of this paper, a few different approaches have been used to quantitatively measure aa-tRNA-dependent transamidation. Precise K_m values were reported for Asp-tRNA^{Asn} by the *Neisseria meningitidis* GatCAB (*27*), with [^{14}C]aspartic acid, and for Asp-tRNA^{Asn} and Glu-tRNA^{Gln} by the *H. pylori* GatCAB, with mischarged ^{32}P76-labeled tRNA(*13*). An electrophoretic assay was also published (*28*), although kinetic results obtained with it have yet to be published. The *N. meningitidis* study used a variation of the method used by Curnow et al. (*4*), while the *H. pylori* study employed a method adapted from work done with aminoacyl-tRNA synthetases (*29*). In another adaptation of the assay by Curnow et al. (*4*), our transamidation experiments were conducted under conditions similar to those used in the ^{32}P assay, with consistent differences being a more acidic pH (7.0), lower ATP concentration (2 mM), and the use of unfractionated tRNA charged with [^{14}C]aspartic acid. Due to these differences, the values of the kinetic parameters that we present below for Asp-tRNA^{Asn} in the absence of ND-AspRS differ from those presented in the detailed study by Sheppard et al. (*13*).

The use of tRNA mischarged with ^{14}C-labeled glutamate or aspartic acid, or of mischarged ^{32}P76-labeled tRNA, allowed detection of the product even with low concentrations of tRNA, but the kinetics revealed that the half-lives of these mischarged aa-tRNAs, and especially their transamidated products, were relatively short (*27*; Figure 4). This problem was resolved by measuring initial rates during periods much shorter than these half-lives. Also, the phenol extraction and ethanol wash steps were omitted because they introduced a high level of variability in asparagine quantification, likely due to erosion of the aa-tRNA pellet. Only in the tests during which aminoacylation and transamidation were done in the same mixture did this result in high levels of unbound [^{14}C]aspartic acid. However, this did not hinder the aa-tRNA deacylation or the chromatographic separation of aspartic acid and asparagine. In tests with phenol/chloroform-extracted Asp-tRNA, the ethanol precipitation steps reduced unbound [^{14}C]aspartic acid to trace amounts (Figure 3, lanes A6, B6, and C6). The use of a standard curve to quantify asparagine allowed us to obtain precise measurements with unfractionated tRNA.

Effects of GatCAB and ND-AspRS on aminoacyl-tRNA half-lives. Deacylation of Asp-tRNA^{Asn} and Asn-tRNA^{Asn} was measured in duplicate by a filter paper and TCA assay (Figure 4). *E. coli* tRNA^{Asp} and tRNA^{Asn} were contaminants but did not contribute more than 20% or 15% of all aa-tRNA formed, respectively. In the absence of GatCAB, Asp-tRNA^{Asn} had a half-life of 136 ± 10 min, which decreased

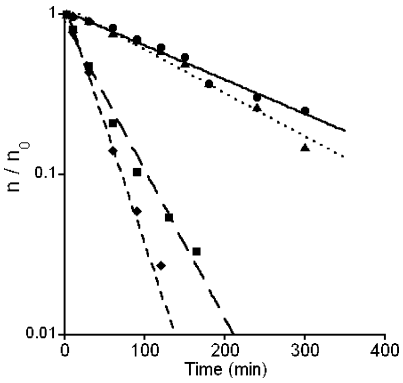

FIGURE 4: Asp-tRNA^{Asn} was prepared as described under Materials and Methods and added to the reaction mixture used for the transamidase assay. Half-lives were determined by a filter paper and TCA precipitation assay (see Materials and Methods). The data are presented as the fraction of aa-tRNA remaining (n/n_0) as a function of the incubation time at 37 °C. The longest half-life was that of Asp-tRNA^{Asn} in the absence of GatCAB, which was 136 ± 10 min (●). This was followed by Asp-tRNA^{Asn} in the presence of GatCAB but in the absence of glutamine, with a half-life of 123 ± 6 min (▲). With L-glutamine present to allow a rapid transformation of Asp-tRNA^{Asn} into Asn-tRNA^{Asn}, the half-life was 20 ± 0.4 min (◆). When ND-AspRS was added to this reaction mixture, the half-life increased to 32 ± 1 min (■). Curve-fitting was done with the standard exponential equation: $n/n_0 = e^{-kt}$, where n/n_0 is the remaining fraction of aa-tRNA, k is the decay constant, and t is time. All reactions were performed in duplicate.

to 123 ± 6 min when in the presence of GatCAB, which was inactive due to the absence of L-glutamine. The fact that this difference is not significant (Figure 4) indicates that GatCAB does not stabilize the ester linkage of Asp-tRNA^{Asn} under these conditions. When glutamine was added in another experiment, the 250 nM concentration of GatCAB allowed a rapid transformation of Asp-tRNA^{Asn} into Asn-tRNA^{Asn}, which had a half-life of 20 ± 0.4 min. When 800 nM *H. pylori* ND-AspRS was added, the half-life of Asn-tRNA^{Asn} increased to 32 ± 1 min.

Determining the tRNA^{Asn} Concentration of an Unfractionated tRNA Stock. The aminoacylation and transamidation assay was used to quantify tRNA^{Asn} concentrations in unfractionated tRNA stocks that contained *E. coli* tRNA^{Asn}, *E. coli* tRNA^{Asp}, and RNA contaminants in addition to the overproduced *H. pylori* tRNA^{Asn}. A 5 μM aliquot of this stock as determined by absorbance at 260 nm was incubated with 800 nM *P. aeruginosa* ND-AspRS for 90 min, which ensured complete aminoacylation. GatCAB was then added as described under Materials and Methods, allowing the transformation of *E. coli* and *H. pylori* Asp-tRNA^{Asn} into Asn-tRNA^{Asn}. The value of the transamidation plateau was then compared to the total concentration (A_{260}) to obtain the tRNA^{Asn} percentage of the unfractionated solution (Figure 5).

Effect of ND-AspRS on K_m Values for Asp-tRNA^{Asn}. The GatCAB transamidation assay, described above, allowed us to determine the K_m and k_{cat} values for Asp-tRNA^{Asn} in the absence of ND-AspRS (Figure 6). We then used this same method to determine those same kinetic values in the presence of *P. aeruginosa* and *H. pylori* ND-AspRS, as well as in the presence of an equivalent concentration of bovine serum albumin (BSA) as a control. These results, presented in Figure 6, indicate that the ND-AspRS concentrations used decreased the K_m of GatCAB for Asp-tRNA^{Asn}. It was

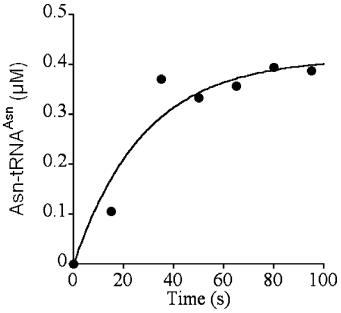

FIGURE 5: Determination of tRNA^{Asn} concentrations with a transamidation plateau. The assay was performed in the basic reaction mixture containing 5 μM unfractionated tRNA enriched with *H. pylori* tRNA^{Asn} (see Materials and Methods). ND-AspRS was used at a concentration of 300 nM, and the reaction mixture was then incubated for 90 min. GatCAB was then added at a concentration of 250 nM in order to use all available substrate before deacylation of the substrate or of the product could become significant (●). The resulting Asn-tRNA^{Asn} plateau corresponded to the tRNA^{Asn} concentration. This concentration was determined from a standard product formation curve: $P(t) = S_0(1 - e^{-kt})$, where k is the kinetic constant for product formation, t is time, and S_0 is the initial substrate (or tRNA^{Asn}) concentration as calculated by best fit. The ratio of tRNA^{Asn} usable by GatCAB against that of total RNA as measured by absorbance at 260 nm was determined to be 8.25% for this particular stock.

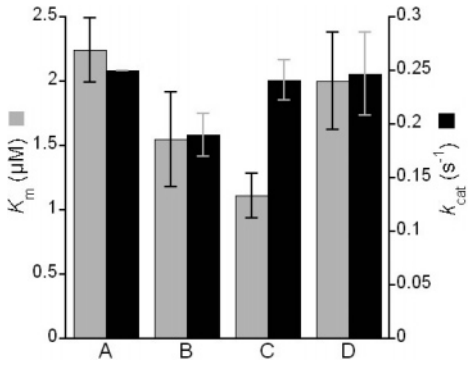

FIGURE 6: ND-AspRS increases *H. pylori* GatCAB affinity for Asp-tRNA^{Asn}. K_m values for Asp-tRNA^{Asn} (gray bars) and k_{cat} values (black bars) were determined in the transamidation reaction, in the absence of ND-AspRS (A) and in the presence of 800 nM ND-AspRS from *P. aeruginosa* (B) and *H. pylori* (C). An experiment was also performed in the presence of an equivalent amount of BSA (52.35 μg/mL) but in the absence of ND-AspRS (D). All experiments were performed in duplicate. In the absence of ND-AspRS, K_m was 2.24 μM, while k_{cat} was 0.25 s^{-1}. In the presence of *P. aeruginosa* and *H. pylori* ND-AspRS, K_m was 1.4 and 2.0 times lower, respectively. In the presence of BSA, K_m was reduced only by a factor of 1.1. In all cases, k_{cat} did not change significantly except for *P. aeruginosa* ND-AspRS, which had a k_{cat} 1.3 times lower than when ND-AspRS was absent.

recently shown that *E. coli* tRNA^{Asn} can be transamidated by *H. pylori* AdT (*23*), and this was our finding as well (results not shown). The values obtained for *H. pylori* Asp-tRNA^{Asn} are not significantly affected by the presence of *E. coli* Asp-tRNA^{Asn} since only approximately 10−15% of tRNA^{Asn} that was used is from *E. coli;* moreover, recent information suggests that differences between *H. pylori* and *E. coli* tRNA^{Asn} are likely to be of minimal importance to enzyme binding (*10*, *27*).

H. pylori ND-AspRS Binds Asp-tRNA. Under conditions very similar to those used for the transamidase activity assay (see Materials and Methods), *H. pylori* ND-AspRS was able to bind significantly more Asp-tRNA than did BSA, which

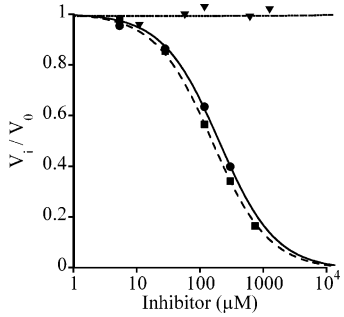

FIGURE 7: Competitive inhibition of *H. pylori* AdT by aspartycin (●) and glutamycin (■). Reactions were performed in the basic reaction mixture, with 0.40 μM Asp-tRNA^{Asn} and 6 nM AdT. V_0 is the uninhibited rate of product formation, V_{max} is the maximum rate, S is the substrate concentration, V_i is the inhibited rate, and I is the inhibitor concentration: according to Michaelis−Menten, $V_0 = (V_{max}S)/(S + K_m)$, while competitive inhibition states that $V_i = (V_{max}S)/\{S + K_m[1 + (I/K_i)]\}$. Therefore, if S is equal to K_m, V_i/V_0 is equal to $2/[2 + (I/K_i)]$; this equation was used for these curve fittings. Inhibition was competitive in the case of aspartycin and glutamycin, having K_i values of 134 μM and 105 μM respectively. Asp-KP (▼) did not inhibit AdT, even at concentrations up to 1 mM.

was used as a control (see Discussion). When no protein was present in the reaction mixture, only 2.7% ± 0.5% of 207 nM Asp-tRNA was retained on the nitrocellulose filters, while in the presence of 800 nM BSA, 4.33% ± 0.13% was retained. GatCAB at concentrations of 400 and 1000 μM bound 12.76% ± 0.93% and 17.8% ± 0.35% of Asp-tRNA, respectively. A concentration of 800 nM *H. pylori* ND-AspRS bound 10.58% ± 0.85% of Asp-tRNA, a proportion significantly higher than what we detected with BSA or no protein at all.

Novel Inhibitors of the Transamidation Reaction Catalyzed by GatCAB. Asp-KP, an analogue of the β-phosphoryl-Asp-tRNA^{Asn} intermediate (Figure 2), did not inhibit GatCAB up to a concentration of 1 mM (Figure 7). Aspartycin and glutamycin, analogues of the 3′-ends of Asp-tRNA and Glu-tRNA, respectively (Figure 1), did inhibit that reaction competitively with respect to Asp-tRNA^{Asn}, as indicated by excellent curve-fitting with the competitive inhibition equation (Figure 7), with K_i values of 134 μM and 105 μM, respectively.

Aspartycin Is Not a Substrate of AdT. The similarity between the two inhibitors and the corresponding misacylated tRNA substrates prompted us to investigate whether they could be transamidated by GatCAB. Samples were prepared in which high concentrations of this enzyme (450 nM) and of aspartycin (1 mM) had been incubated for 5 h at 37 °C in the basic reaction mixture; aspartic acid was omitted, and 25 mM NH_4Cl was added to enable a bypass of the glutaminase activity. These samples were then fractionated by reverse-phase chromatography and analyzed by mass spectrometry (see Materials and Methods). Since the amidation of aspartycin decreases its molecular mass by 1 unit at the low pH used for these experiments, aspartycin and its amidated product should be easily distinguished by MS. While unmodified aspartycin was easily detected, there were no signs of inhibitor modification by the enzyme (Figure 8).

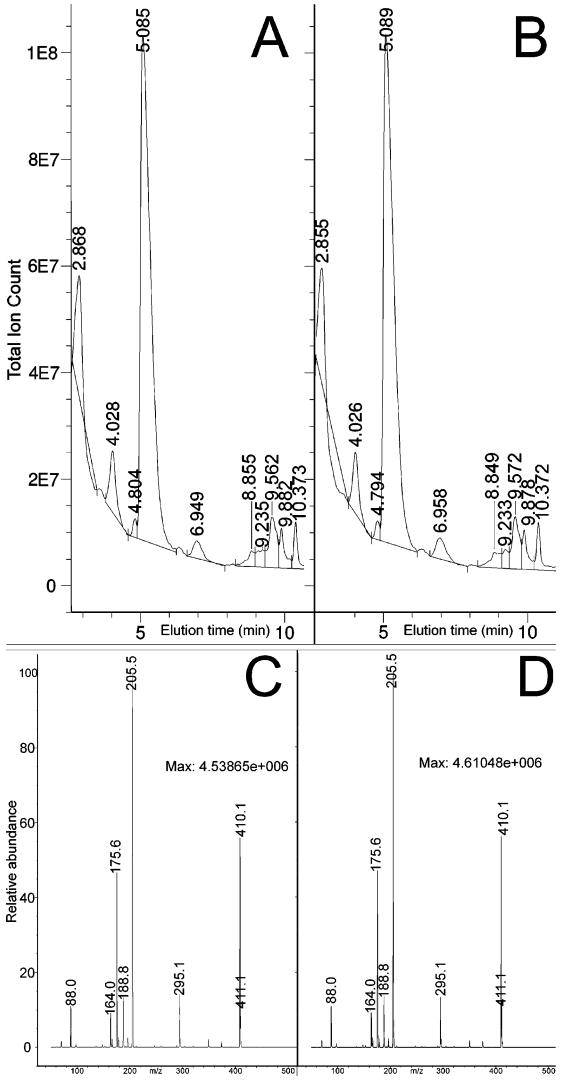

FIGURE 8: Aspartycin is not a substrate for GatCAB. Samples containing 1 mM aspartycin, in the basic reaction mixture supplemented with 25 mM NH_4Cl, were incubated with 0 or 450 nM GatCAB for 5 h at 37 °C. Separation of the samples by reverse-phase chromatography (see Materials and Methods) was conducted before analysis by mass spectrometry. Aspartycin and its putative amidated product have similar hydrophobicities and therefore are expected to be eluted in the same region. In the absence of GatCAB, aspartycin was eluted after approximately 5.1 min (A). This peak was also present in the sample containing GatCAB (B), and there was no reduction in its importance nor formation of new peaks in the region. In panel C, we see that the 5.1 min elution peak contained aspartycin ions with a single positive charge (m/z = 410.1) and with two positive charges (m/z = 205.5). The spectral data in panel D are identical to the data in panel C, showing no decrease in the abundance of either aspartycin ion and no new peaks corresponding to the putative modified aspartycin. This putative amidated aspartycin, under the acidic conditions used, would have a mass that is lesser than that of aspartycin by 1 unit; this difference being detectable in the performed analysis, we conclude that aspartycin cannot be modified by GatCAB.

DISCUSSION

The original objective of this study was to identify aa-tRNA analogues that would inhibit GatCAB competitively. The aminoacylation and transamidation assay was convenient for the testing of these analogues, as discussed below. To measure the K_i values for these analogues, we first sought to determine the K_m and k_{cat} for Asp-tRNA^{Asn}. Since the inhibitor tests are conducted in the presence of ND-AspRS, we considered that there could be some form of interaction between ND-AspRS and GatCAB, as was suggested by molecular modeling for ND-GluRS and GatDE (*12*). This model, which shows that binding of ND-GluRS to GatDE is unobstructed and possible, also indicates that the presence of an AspRS-like domain on GatDE would prevent the docking of ND-AspRS. As GatCAB does not contain this AspRS-like domain and is able to transamidate both Glu-tRNA^{Gln} and Asp-tRNA^{Asn}, the existence of a ND-AspRS/GatCAB complex is conceivable. To explore this possibility, we decided to determine the kinetic parameters for Asp-tRNA^{Asn} in the transamidase reaction in the absence of ND-AspRS, as well as in the presence of ND-AspRS from both *P. aeruginosa* and *H. pylori*. As a control, K_m and k_{cat} values were also determined for Asp-tRNA^{Asn} in the presence of BSA. These experiments revealed that the presence of ND-AspRS from *H. pylori* reduces the K_m for Asp-tRNA^{Asn} by a factor of 2.0, while ND-AspRS from *P. aeruginosa* reduced the K_m by a factor of 1.4 (Figure 6). The transamidation assay we used to determine these values minimized the effect of deacylation, which was primarily of concern for Asn-tRNA^{Asn} and its 20 min half-life, by reducing reaction times to 2 min or less. Unbound aspartic acid, which was the result of whatever deacylation may have occurred with Asp-tRNA, was not found in concentrations high enough to allow significant reacylation to occur in reaction mixtures containing added ND-AspRS. The control experiment performed with BSA indicates that excluded volume effects are not responsible for the drop in K_m values seen in the presence of ND-AspRS. We thus propose that a transfer of Asp-tRNA^{Asn} from ND-AspRS onto GatCAB decreases the K_m for Asp-tRNA^{Asn} through increased interactions made possible by the synthetase. This is consistent with the fact that ND-AspRS binds about half as much Asp-tRNA as does GatCAB. The observed binding of [^{14}C]Asp-tRNA to GatCAB cannot be attributed solely to Asp-tRNA^{Asp}, as the unfractionated stock we used contained about 4 times more tRNA^{Asn} than tRNA^{Asp}, while ND-AspRS bound approximately half as much Asp-tRNA as does GatCAB. Considering that the K_m of *H. pylori* ND-AspRS for its homologous tRNA^{Asp} is 0.77 μM (*23*) and that the concentration of *E. coli* Asp-tRNA^{Asp} in our binding assays was about 0.05 μM, it is very unlikely that the Asp-tRNA bound could be mainly composed of Asp-tRNA^{Asp}.

These facts are compatible with channeling of Asp-tRNA^{Asn} from ND-AspRS to GatCAB. If this binding rendered Asp-tRNA^{Asn} unusable by GatCAB, we should have seen an increase in our K_m values, rather than a decrease. As we did not succeed at isolating a ND-AspRS/GatCAB complex (results not shown), and as no other investigator reported the detection of such a complex, we suggest that this mechanism could involve the formation of a transient ternary complex. If short-lived, this complex would allow for a more efficient transit of tRNA^{Asn} through the aspartylation and transamidation steps. A longer-lasting complex could also exist, involving contact of ND-AspRS from the acceptor stem to the anticodon loop on the variable loop face of Asp-tRNA^{Asn} (*30*), as well as contact between the acceptor arm and GatCAB (*10*). While our results suggest that the binding of Asp-tRNA^{Asn} by ND-AspRS or both enzymes may be weaker than the binding of canonical aa-tRNAs (*31*) or even misacylated aa-tRNAs (*32*) by EF-Tu, the obstruction

of parts of the Asp-tRNA^{Asn} acceptor arm, especially by GatCAB, could prevent the binding of EF-Tu. It is interesting to note that GatCAB appears to bind aa-tRNA in a way similar to EF-Tu, making contact with the acceptor arm and ester bond region (*33*). In conjunction with GatCAB, ND-AspRS increases the stability of Asn-tRNA^{Asn} (Figure 4), like EF-Tu does for all canonical aa-tRNAs. Asp-tRNA^{Asn} therefore might not be released by ND-AspRS but rather taken directly to GatCAB, forming a complex that prevents the docking of EF-Tu and offers stabilization of the ester bond.

The stability of the aminoacyl ester bonds of aminoacyl-tRNAs (aa-tRNA) depends on the nature of the amino acid but not on that of tRNA [*34*, *35*; reviewed by Söll and Schimmel (*36*)]. The half-lives of *E. coli* Asp-tRNA^{Asp} and Asn-tRNA^{Asn} at 37 °C are identical (*34*), but in the case of the two GatCAB-containing bacteria *H. pylori* and *N. meningitidis* (*27*), the half-life of Asn-tRNA^{Asn} is much shorter than that of Asp-tRNA^{Asn} (Figure 4). These results are in accordance with the documented role of GatCAB in synthesizing asparagine in organisms that are, or were at one point, devoid of an asparagine synthase (see the introduction). The above-mentioned ternary complex might also slow the uptake of Asn-tRNA^{Asn} by EF-Tu, allowing additional asparagine to be released.

At the onset of this study, we expected Asp-tRNA^{Asn} to have the shorter half-life of the two aa-tRNAs, as it could have then benefited from a protection of the ester bond between its amino acid and tRNA moieties, provided by its binding of ND-AspRS. This protection, which might have been similar to the one described above, could have explained the lower K_m values seen for Asp-tRNA^{Asn} with GatCAB in the presence of ND-AspRS. As Asp-tRNA^{Asn} has a half-life of 136 min under the conditions tested (Figure 4), this putative stabilization remains possible but seems unnecessary. The presence of ND-AspRS in this experiment could not lead to tRNA aspartylation because Asp-tRNA was prepared in another reaction mixture and purified before being used, resulting in an insufficient amount of aspartic acid. The presence of active GatCAB in the reaction mixture also ensures that any amino acid freed by deacylation would be Asn and therefore not usable by ND-AspRS. Given its role in asparagine synthesis in many organisms, it is possible that the deacylation of Asn-tRNA^{Asn} has a higher chance of occurring during its separation from GatCAB than afterward. Further experiments are needed to verify this possibility, but the influence of ND-AspRS on the half-life of Asn-tRNA^{Asn} remains indicative of a contact between this enzyme and GatCAB. A practical aspect of these results is that when potential inhibitors are tested in our combined aminoacylation and transamidation assay, the K_m for Asp-tRNA^{Asn} that must be used is the one obtained in the presence of *P. aeruginosa* ND-AspRS.

Glutamycin, an analogue of the 3′-end of glutamyl-tRNA, was first designed as a potential inhibitor of the glutamyl-tRNA reductase (GluTR) (*21*). Although it was only a weak inhibitor of GluTR (K_i on the order of 1.5 mM), it was very useful in facilitating GluTR crystallization, and its localization on the enzyme at 1.9 Å resolution provided information about GluTR mechanism (*19*); in particular, modeling based on the well-defined location of glutamycin allowed the positioning of the acceptor stem of *T. thermophilus* tRNA^{Glu} into the active site and revealed an extensive GluTR/glutamyl-tRNA interface. This model and the weak binding of glutamycin to GluTR indicate that this enzyme has only a few contacts with the glutamyl-adenosine at the 3′-end of glutamyl-tRNA and that it recognizes this substrate mostly by other structural elements of this tRNA. The situation is quite different in the case of the interaction of this analogue with GatCAB: it inhibits it more strongly ($K_i = 0.105$ mM, which is about 14-fold more efficient than for GluTR). This result is compatible with the fact that GatCAB has two different aminoacyl-tRNA substrates whose nucleotide sequences differ significantly, a situation that may have led to more interactions with their common 3′-terminal features. The absence of AdT inhibition by the Asp-KP analogue (Figure 2), which lacks the adenosyl module, also suggests that a significant portion of binding occurs at the 3′ end of the tRNA, although further experimentation is needed to determine to what extent its structural differences with the β-phosphoaspartate side chain affect its binding.

The part of aspartycin that is similar to Asp (Figure 1; the only differences are a NH replacing one of the O of the α-carboxy of Asp and two methyl residues on the adenine base) has a side chain identical to that of aspartic acid, and thus its β-carboxyl group could conceivably be phosphorylated and then transamidated by AdT. Our attempts at detecting these modified forms of aspartycin revealed that this inhibitor is not a substrate of AdT (Figure 8), which indicates that its β-carboxyl group is not positioned in the active site exactly as is that of Asp-tRNA^{Asn}. This suggests that the proposed interactions between the tRNA acceptor arm and GatB have a role not only in substrate binding but also in ensuring the proper orientation of the 3′ end in the active site (*10*).

ACKNOWLEDGMENT

We thank Dr Alain Garnier and Lise Lemieux for the LCMS analyses. We are also thankful to Dr Dieter Söll and Dr Tamara Hendrickson for providing us with the overproducing strains for *H. pylori* GatCAB, tRNA^{Asn} and ND-AspRS.

REFERENCES

1. Ataide, S. F., and Ibba, M. (2006) Small molecules: big players in the evolution of protein synthesis, *ACS Chem. Biol. 1*, 285−297.
2. Hendrickson, T. L., and Schimmel, P. (2003) Transfer RNA-dependent amino acid discrimination by aminoacyl-tRNA synthetases, in *Translation Mechanisms* (Lapointe, J., and Brakier Gingras, L., Eds.) pp 34−64, Landes Biosciences/Eurekah.com and Kluwer Academic/Plenum Publishers.
3. Ruan, B., and Söll, D. (2005) The bacterial YbaK protein is a Cys-tRNA^{Pro} and Cys-tRNA^{Cys} deacylase, *J. Biol. Chem. 280*, 25887−25891.
4. Curnow, A. W., Hong, K., Yuan, R., Kim, S., Martins, O., Winkler, W., Henkin, T. M., and Soll, D. (1997) Glu-tRNA^{Gln} amidotransferase: a novel heterotrimeric enzyme required for correct decoding of glutamine codons during translation, *Proc. Natl. Acad. Sci. U.S.A. 94*, 11819−11826.
5. Becker, H. D., and Kern, D. (1998) *Thermus thermophilus*: a link in evolution of the tRNA-dependent amino acid amidation pathways. *Proc. Natl. Acad. Sci. U.S.A. 95*, 12832−12837.
6. Curnow, A. W., Tumbula, D. L., Pelaschier, J. T., Min, B., and Soll, D. (1998) Glutamyl-tRNA^{Gln} amidotransferase in *Deinococcus radiodurans* may be confined to asparagine biosynthesis, *Proc. Natl. Acad. Sci. U.S.A. 95*, 12838−12843.

7. Min, B., Pelaschier, J. T., Graham, D. E., Tumbula-Hansen, D., and Soll, D. (2002) Transfer RNA-dependent amino acid biosynthesis: an essential route to asparagine formation, *Proc. Natl. Acad. Sci. U.S.A. 99*, 2678−2683.
8. Schell, M. A., Karmirantzou, M., Snel, B., Vilanova, D., Berger, B., Pessi, G., Zwahlen, M. C., Desiere, F., Bork, P., Delley, M., Pridmore, R. D., and Arigoni, F. (2002) The genome sequence of *Bifidobacterium longum* reflects its adaptation to the human gastrointestinal tract, *Proc. Natl. Acad. Sci. U.S.A. 99*, 14422−14427.
9. Ibba, M., Becker, H. D., Stathopoulos, C., Tumbula, D. L., and Söll, D. (2000) The adaptor hypothesis revisited. *Trends Biochem. Sci. 25*, 311−316.
10. Nakamura, A., Yao, M., Chimnaronk, S., Sakai, N., and Tanaka, I. (2006) Ammonia channel couples glutaminase with transamidase reactions in GatCAB, *Science 312*, 1954−1958.
11. Schmitt, E., Panvert, M., Blanquet, S., and Mechulam, Y. (2005) Structural basis for tRNA-dependent amidotransferase function, *Structure 13*, 1421−1433.
12. Oshikane, H., Sheppard, K., Fukai, S., Nakamura, Y., Ishitani, R., Numata, T., Sherrer, R. L., Feng, L., Schmitt, E., Panvert, M., Blanquet, S., Mechulam, Y., Soll, D., and Nureki, O. (2006) Structural basis of RNA-dependent recruitment of glutamine to the genetic code, *Science 312*, 1950−1954.
13. Sheppard, K., Akochy, P. M., Salazar, J. C., and Soll, D. (2007) The *Helicobacter pylori* amidotransferase GatCAB is equally efficient in glutamine-dependent transamidation of Asp-tRNA^{Asn} and Glu-tRNA^{Gln}, *J. Biol. Chem. 282*, 11866−11873.
14. Rinehart, J., Krett, B., Rubio, M. A., Alfonzo, J. D., and Söll, D. (2005) *Saccharomyces cerevisiae* imports the cytosolic pathway for Gln-tRNA synthesis into the mitochondrion, *Genes Dev. 19*, 583−592.
15. Kern, D., Roy, H., and Becker, H. D. (2005) Asparaginyl-tRNA synthetase, in *The Aminoacyl-tRNA Synthetases* (Ibba, M., Francklyn, C., and Cusack, S., Eds.) pp 193−209, Eurekah.com/Landes Bioscience, Georgetown, TX.
16. Decicco, C. P., Nelson, D. J., Luo, Y., Shen, L., Horiuchi, K. Y., Amsler, K. M., Foster, L. A., Spitz, S. M., Merrill, J. J., Sizemore, C. F., Rogers, K. C., Copeland, R. A., and Harpel, M. R. (2001) Glutamyl-γ-boronate inhibitors of bacterial Glu-tRNA^{Gln} amidotransferase, *Bioorg. Med. Chem. Lett. 11*, 2561−2564.
17. Harpel, M. R., Horiuchi, K. Y., Luo, Y., Shen, L., Jiang, W., Nelson, D. J., Rogers, K. C., Decicco, C. P., and Copeland, R. A. (2002) Mutagenesis and mechanism-based inhibition of *Streptococcus pyogenes* Glu-tRNA^{Gln} amidotransferase implicate a serine-based glutaminase site, *Biochemistry 41*, 6398−6407.
18. Horiuchi, K. Y., Harpel, M. R., Shen, L., Luo, Y., Rogers, K. C., and Copeland, R. A. (2001) Mechanistic studies of reaction coupling in Glu-tRNA^{Gln} amidotransferase, *Biochemistry 40*, 6450−6457.
19. Moser, J., Schubert, W. D., Beier, V., Bringemeier, I., Jahn, D., and Heinz, D. W. (2001) V-shaped structure of glutamyl-tRNA reductase, the first enzyme of tRNA-dependent tetrapyrrole biosynthesis, *EMBO J. 20*, 6583−6590.
20. Rudisill, D. E., and Whitten, J. P. (1994) Synthesis of (*R*)-4-Oxo-5-phosphononorvaline, an *N*-Methyl-D-aspartic Acid Receptor Selective β-Keto Phosphonate, *Synthesis 1994*, 851−854.
21. Moser, J., Lorenz, S., Hubschwerlen, C., Rompf, A., and Jahn, D. (1999) *Methanopyrus kandleri* glutamyl-tRNA reductase, *J. Biol. Chem. 274*, 30679−30685.
22. Akochy, P. M., Bernard, D., Roy, P. H., and Lapointe, J. (2004) Direct glutaminyl-tRNA biosynthesis and indirect asparaginyl-tRNA biosynthesis in *Pseudomonas aeruginosa* PAO1, *J. Bacteriol. 186*, 767−776.
23. Chuawong, P., and Hendrickson, T. L. (2006) The nondiscriminating aspartyl-tRNA synthetase from *Helicobacter pylori*: anticodon-binding domain mutations that impact tRNA specificity and heterologous toxicity, *Biochemistry 45*, 8079−8087.
24. Studier, F. W. (2005) Protein production by auto-induction in high density shaking cultures, *Protein Expression Purif. 41*, 207−234.
25. Yarus, M., and Berg, P. (1970) On the properties and utility of a membrane filter assay in the study of isoleucyl-tRNA synthetase, *Anal. Biochem. 35*, 450−465.
26. Roy, H., Becker, H. D., Mazauric, M. H., and Kern, D. (2007) Structural elements defining elongation factor Tu mediated suppression of codon ambiguity, *Nucleic Acids Res. 35*, 3420−3430.
27. Bailly, M., Giannouli, S., Blaise, M., Stathopoulos, C., Kern, D., and Becker, H. D. (2006) A single tRNA base pair mediates bacterial tRNA-dependent biosynthesis of asparagine, *Nucleic Acids Res. 34*, 6083−6094.
28. Cathopoulis, T. J., Chuawong, P., and Hendrickson, T. L. (2007) A thin-layer electrophoretic assay for Asp-tRNA^{Asn}/Glu-tRNA^{Gln} amidotransferase, *Anal. Biochem. 360*, 151−153.
29. Wolfson, A. D., Pleiss, J. A., and Uhlenbeck, O. C. (1998) A new assay for tRNA aminoacylation kinetics, *RNA 4*, 1019−1023.
30. Moulinier, L., Eiler, S., Eriani, G., Gangloff, J., Thierry, J. C., Gabriel, K., McClain, W. H., and Moras, D. (2001) The structure of an AspRS−tRNA^{Asp} complex reveals a tRNA-dependent control mechanism, *EMBO J. 20*, 5290−5301.
31. LaRiviere, F. J., Wolfson, A. D., and Uhlenbeck, O. C. (2001) Uniform binding of aminoacyl-tRNAs to elongation factor Tu by thermodynamic compensation, *Science 294*, 165−168.
32. Asahara, H., and Uhlenbeck, O. C. (2005) Predicting the binding affinities of misacylated tRNAs for *Thermus thermophilus* EF-Tu·GTP, *Biochemistry 44*, 11254−11261.
33. Nissen, P., Kjeldgaard, M., Thirup, S., Clark, B. F., and Nyborg, J. (1996) The ternary complex of aminoacylated tRNA and EF-Tu-GTP. Recognition of a bond and a fold, *Biochimie 78*, 921−933.
34. Hentzen, D., Mandel, P., and Garel, J. P. (1972) Relation between aminoacyl-tRNA stability and the fixed amino acid, *Biochim. Biophys. Acta 281*, 228−232.
35. Strickland, J. E., and Jacobson, K. B. (1972) Effects of amino acid structure, ionic strength, and magnesium ion concentration on rates of nonenzymic hydrolysis of aminoacyl transfer ribonucleic acid, *Biochemistry 11*, 2321−2323.
36. Söll, D., and Schimmel, P. R. (1974) Aminoacyl-tRNA synthetase, in *The Enzymes* (Boyer, P. D., Ed.) pp 489−538, Academic Press, San Diego, CA.

BI700602N